



HAL
open science

Quantum scattering engineering of quantum well infrared photodetectors in the tunneling regime

Emmanuel Lhuillier, Emmanuel Rosencher, Isabelle Ribet-Mohamed,
Alexandru Nedelcu, Laetitia Doyennette, Vincent Berger

► **To cite this version:**

Emmanuel Lhuillier, Emmanuel Rosencher, Isabelle Ribet-Mohamed, Alexandru Nedelcu, Laetitia Doyennette, et al.. Quantum scattering engineering of quantum well infrared photodetectors in the tunneling regime. *Journal of Applied Physics*, 2010, 108, pp.113707-113707. 10.1063/1.3514155 . hal-01438638

HAL Id: hal-01438638

<https://hal.science/hal-01438638>

Submitted on 23 Dec 2020

HAL is a multi-disciplinary open access archive for the deposit and dissemination of scientific research documents, whether they are published or not. The documents may come from teaching and research institutions in France or abroad, or from public or private research centers.

L'archive ouverte pluridisciplinaire **HAL**, est destinée au dépôt et à la diffusion de documents scientifiques de niveau recherche, publiés ou non, émanant des établissements d'enseignement et de recherche français ou étrangers, des laboratoires publics ou privés.

Quantum scattering engineering of quantum well infrared photodetectors in the tunnelling regime

Emmanuel Lhuillier^{1,2}, Emmanuel Rosencher¹, Isabelle Ribet-Mohamed¹, Alexandru Nedelcu³, Laetitia Doyennette², Vincent Berger².

¹ONERA, Chemin de la Hunière, 91761 Palaiseau cedex, France.

²Matériaux et Phénomènes Quantiques, Université Paris 7, Bat. Condorcet, Case 7021, 75205 Paris cedex 13, France.

³Alcatel-Thales III-V Lab, Campus de l'Ecole Polytechnique, 1 Avenue A. Fresnel, 91761 Palaiseau cedex, France.

Abstract

Dark current is shown to be significantly reduced in quantum well infrared photodetectors in the tunneling regime, i.e. at very low temperature, by shifting the dopant impurity layers away from the central part of the wells. This result confirms that the interwell tunneling current is dominated by charged impurity scattering in usual structures. The experimental results are in good quantitative agreement with the proposed theory. This dark current reduction is pushing further the ultimate performances of quantum well infrared photodetectors for the detection of low infrared photon fluxes. Routes to further improvements are briefly sketched.

PACS number(s): 73.63.Hs, 72.10.-d, 85.60.Gz

I. Introduction

Quantum well infrared photodetectors (QWIP) have been extensively used^{1,2} for the detection of low infrared photon flux which is of utmost importance in aerospace applications for instance. Indeed, for such applications, background temperature below 100 K are common which involves a long wavelength infrared detector (typically beyond 15 μm) as well as a dark current electron flux in the detector far below the photon flux which is $\approx 10^{13}$ photons. $\text{cm}^{-2}\text{s}^{-1}$. Such performances can be obtained only at very low temperature, i.e. in the tunnelling regime³. Indeed, the operating temperature for QWIP is generally in the

50 to 75K range⁴ for 10 μ m detectors but in the 35 to 60K range^{4,5} around 15 μ m. These temperatures are a compromise between the level of performance of the detector and the lifetime of the cryogenic cooling device. It has already been demonstrated that for QWIP operating in the VLWIR (very long wavelength infrared), the dark current level is the point on which performance improvements have to be focused. An increase of performance can generally be reached by decreasing the detector temperature. Such an improvement is possible as long as the dark current is dominated by thermionic emission⁶. However, at sufficiently low temperature, the magnitude of the dark current is driven by the residual tunnel coupling between two following wells. The detector performances become independent of the temperature so that the performance improvements require a structure optimization. A decrease of dark current could be obtained by increasing the barrier thickness, but this techniques present limitations that will be discussed at the end of this paper.

II. Principle of the dark current reduction

In a previous paper we have suggested that for VLWIR QWIP operating in the tunnelling regime, the dark current mostly results from the interaction between the electron and the doping ionized impurities⁷. A change in the QWIP doping profile may thus allow a decrease of the dark current. Usually the doping is located in the central part of the well in QWIP. Changing the doping profile has already been proposed in the literature but for different purposes. In order to solve doping segregation problems, Schneider et al^{8,9} have proposed to move the doping away from its central position to the first part of the well. Luna et al^{10,11} suggested to design modulation doped QWIP in order to improve their responsivity. The effect of the doping position on the spectral response has also been studied by Dupont et al¹² for the control of the transition linewidth and by Pan et al¹³ for the possibility to observe forbidden transitions. In this paper, we propose to investigate the influence of the doping position on the magnitude of the dark current. Structures where dark current is divided by a factor of ≈ 2 , *mutatis mutandis*, will be presented.

In order to predict quantitatively the effect of the doping position we developed a hopping transport model^{7,14,15} which includes interaction of the electrons with LO phonon, LA phonon, alloy disorder,

interface roughness and ionized impurities. Wave functions have been calculated in a two wells structure using a two bands k·p method¹⁶ and self consistent Poisson/Schrödinger code⁷.

In long wavelength QWIPs and for moderate electric field, we have demonstrated that the electron ionized interaction is the one which drives the dark current⁷ in the tunnel regime. Dark current reduction may thus result from a reduction of the impurity mediated scattering rate between the ground states of two adjacent wells. It is interesting to consider the ionized impurities scattering rate expression^{17,18}:

$$\Gamma_{II} = \frac{e^4}{8\pi\hbar\epsilon_0^2\epsilon_r^2} \frac{m^*}{\hbar^2} \int dz_i N(z_i) \times \int d\theta \frac{F_{II}(|K_i - K_f|)}{|K_i - K_f|^2}$$

where e is the proton charge, m^* the GaAs

effective mass, \hbar the reduced Planck constant, ϵ_r the GaAs permittivity, z_i the impurity position, $N(z_i)$ the volumic doping profile, K_i and K_f the initial and final wavevectors and θ the angle between the two vectors K_i and K_f . Finally the overlap integral $F_{II}(Q) = \left| \int dz \xi_f^*(z) e^{-Q|z-z_i|} \xi_i(z) \right|^2$ is the form factor of this interaction, which links the geometry of the device to the magnitude of the scattering: ξ_i (resp. ξ_f) is the initial (resp. final) electron envelope wavefunction.

A careful examination of the form factor expression immediately indicates that, because of the overlap integral between ξ_i and ξ_f mediated by the $e^{-Q|z-z_i|}$ term, moving the doping away from the central part of the well will reduce the form factor and the associated dark current. A possible solution would be to localize the doping impurities in the barriers. However, this is liable to i) introduce deep levels into the barrier¹⁹ which will be detrimental to the dark current level and ii) create quantum levels inside the barrier^{20,21}, which is also detrimental to transport properties. In fact this is a major difference with quantum cascade laser²² (QCL) which are generally doped inside the barrier in order to get a sharp gain curve. At the opposite in detector we are interested in obtaining broad spectral shape. We have thus chosen to move the crenel of doping away from a central position of the well to the border of the well. The shift has been chosen towards the surface of the sample rather than towards the substrate in order to avoid a cancellation of the expected effect by doping segregation problems.

III. Experimental realization

We have designed two structures which are expected to differ only by their doping profile. The structure is a forty periods QWIP grown by molecular beam epitaxy. The nominal well width is 6.8 nm, whereas the barrier width is 39 nm. The aluminium content of the barrier is 15.5%. This results in a peak transition around 13.5 μ m. The doping sheet density is the same for the two devices and equals $3 \times 10^{11} \text{cm}^{-2}$. Structure A (reference) is doped in its central third whereas structure B is doped in its last third (surface side), see the top of FIG. 1. Precise measurements of the well width, barrier width and aluminium content have been obtained using X ray diffraction and results are presented in tab. I.

tab. I : Measurements of well width, barrier width and aluminium content using X ray diffraction

Device	A	B
Doping position	Central doping	Shifted doping
Aluminium content (%)	15.6 \pm 0.1	15.5 \pm 0.1
Well width (nm)	6.7 \pm 0.1	6.7 \pm 0.1
Barrier width (nm)	39.2 \pm 0.1	38.9 \pm 0.1

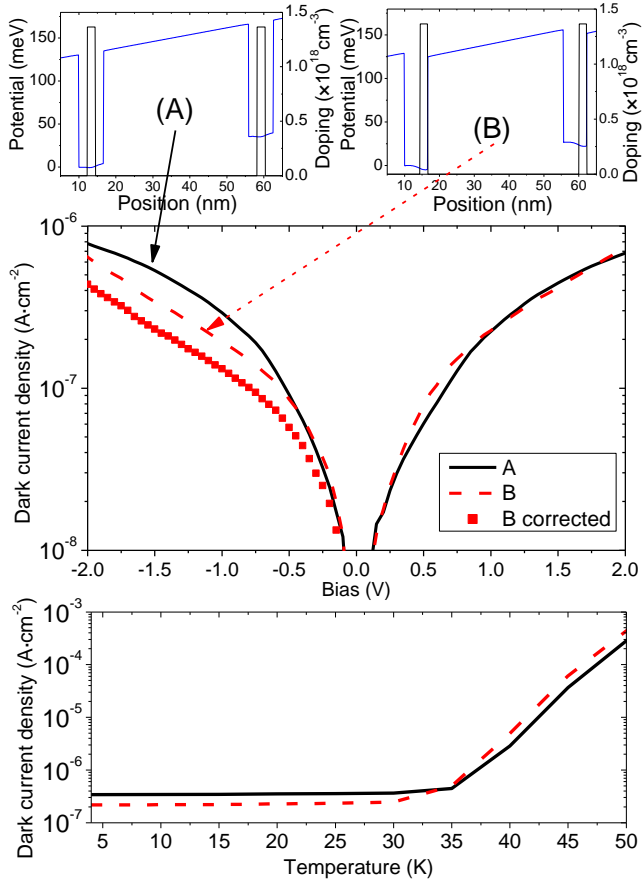


FIG. 1 Upper part: self consistent calculation of the potential profile (blue line) under an electric field of $8\text{kV} \cdot \text{cm}^{-1}$ and the doping profile (black line). Central part: Dark current measurements in the tunneling regime as a function of the applied bias for device A and B, $T=4\text{K}$. The dot curve shows the corrected current for structure B. Lower part: Current as a function of the temperature for the two devices, under a 1.1V bias.

Those samples have been processed into mesas of 50 and $100\mu\text{m}$ sides. The resulting devices are mounted on the cold finger of an helium cryostat. The temperature is regulated with a Lakeshore 331 thermal controller. The current is measured with a sub-femtoamperimeter (Keithley 6430). Spectral measurements have been realized with a Bruker Equinox 55. Quantum efficiency measurements under low infrared flux have been obtained using a double cryostat device: The first cryostat is used to cool the detector while the second cryostat, operated with nitrogen, cools down the blackbody. The numerical aperture of the system is $f/2.8$.

I(V) measurements for the two devices are given on FIG. 1 (central part) in the tunneling regime (T=4 K).

NE MELANGE PAS LES RESULTATS ET LEUR INTERPRETATION!!!!!!!!!!!!

For negative bias, we observe a distinct decrease of the dark current for the shifted doping sample while an almost unnoticeable effect is visible for positive bias . This is in agreement with theoretical expectation. Indeed, for negative bias, the electric field tends to localize the wave function at the opposite of the doping, decreasing the overlap integral (see the blue dotted curve of FIG. 2). On the contrary for positive bias, the electric field moves the electron wave function closer to the doping which tends to increase the form factor, see also FIG. 2. The effect is nevertheless smaller than for positive bias. This decrease comes from the fact that the Stark effect of the wave function is partly counterbalanced by the shift of the doping. We should also notice that the effect on the dark current is smaller than the effect on the form factor due to the effect of the other interaction.(incompréhensible: on le garde?)

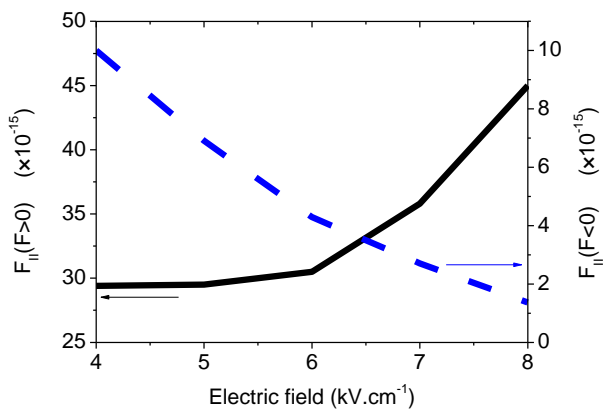


FIG. 2 Form factor for the electron ionized impurities interaction as a function of the electric field for positive and negative electric field. The exchanged momentum is taken equal to 10^8m^{-1} .

FIG. 1 (lower part) shows the dark current as a function of the temperature. At high temperature the reference device presents the lowest current. This results from the difference of confinement of the electron. Indeed spectral measurements, presented on

FIG. 3, show a lower peak energy for the reference device which indicates a higher confinement.

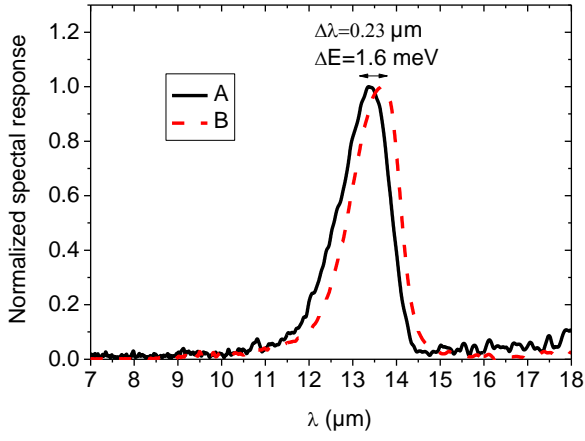


FIG. 3 Spectral measurements for devices A and B, under -1V. The period of the coupling grating is $4.2\mu\text{m}$.

Such a result is confirmed by X-Ray measurements, see tab. I, since the reference presents larger and higher barriers. Due to this composition fluctuation the activation energy is smaller for the reference sample which leads to a reduced dark current for this device when it operates in its thermionic regime. At low temperature, the B device is the one with the smaller dark current, in spite of this lower confinement. The dark current reduction is of 30% in the $-1.5\text{V} \rightarrow -1\text{V}$ range of bias, which is quite close to the expected decrease. To have an idea of the current which we may have obtained in the case where the two samples only differed by their doping position, we plot, on FIG. 1, the experimental current multiplied by the ratio of the tunnelling probability for structures A and B, thus we expect to have corrected the effect linked to the difference in the barrier size. Its expression is given by:

$$J_{corrected} = J_{experimental} \times \frac{P(E_1(A))}{P(E_1(B))}$$

where E_1 is the fundamental level energy and P is given by the WKB approximation²³

$$P(E) = \exp\left(-\frac{4\sqrt{2m_b^*}}{3F\hbar} \left[(Vb - E)^{3/2} - (Vb - eFL_b - E)^{3/2} \right]\right)$$

Thus the corrected effect of the shift of the doping is a 50% decrease of the tunneling dark current.

Finally using 300K absorption measurements, see FIG. 4, we have checked that the absorption is similar for the two devices, which means that the doping levels are very close. Thus we do not expect that the dark current decrease results from a change of the Fermi energy associated to the doping level. **Thus, in spite of the lower confinement, the optimized device presents a reduced dark current.**(encore? Pourquoi encore et là?)

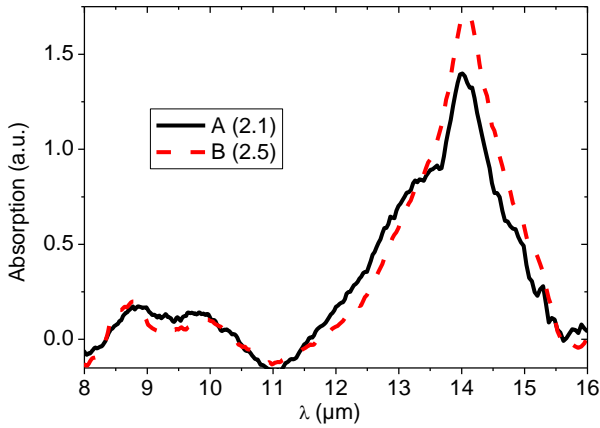


FIG. 4 : 300K absorption spectrum. In parenthesis, in the legend, the value of the integral of each spectrum.

Using the parameters obtained by X-Ray diffraction we can quantitatively compare the theoretical interwell scattering rates with the experimental datas. The experimental interwell scattering rates are

obtained from the expression $\Gamma = \frac{J}{e \cdot n_{2D}}$ where J is the current density and n_{2D} the sheet carrier density.

We also assume that the electric field is constant over the whole structure. We obtained a reasonable agreement for the dark current reduction value between theory and experimental data, see FIG. 5. The difference of the shape of the curves may result from electric field inhomogeneities.

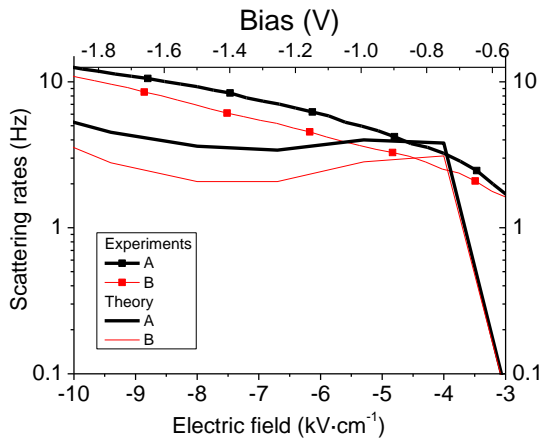


FIG. 5: Experimental and theoretical scattering rates as a function of the applied bias. The theoretical current has been obtained for a doping of $n_{2D}=5\times 10^{11}\text{cm}^{-2}$.

Finally, the external quantum efficiency is almost the same for the two devices: 13.6% for device A and 11.5% for device B, under -2V.

IV. Further improvements

It is possible to further increase this reduction of the dark current. Indeed, for the B structure, the shape of the energy band profile is affected by the electrostatic reconfiguration. A self consistent evaluation of the energy band profile (EBP) is shown FIG. 1. Keeping all growth parameters constant (well and barrier width, aluminium content) the change of the EBP, due to the shift of the doping position, increases the overlap $\langle \Psi_n | \Psi_{n+1} \rangle$ between the ground states by a factor three (with Ψ_n is the ground state wave function of the n^{th} well). The matrix element associated with ionized impurities $\langle \Psi_n | \frac{e^2}{4\pi\epsilon_0\epsilon_r r} | \Psi_{n+1} \rangle$ is reduced but at the same time the matrix elements associated with other interactions raise. Consequently it will be much more favourable to build a symmetric doping profile. For this we can split the crenel of doping in two smaller crenels, each one being located on the edge of the well. FIG. 6 shows a possible design for this doping profile. However such a sample may be limited by the doping segregation.

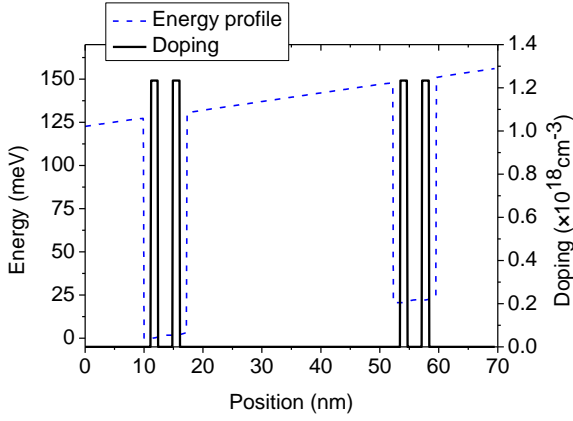


FIG. 6 Possible optimized energy band and doping profile.

V. Range of interest

Low infrared photon flux applications are generally interested in detectors with a very low dark current in order to avoid that the read out circuit capacitance was filled with non photo-electron. To reach this goal the usual solution deals with the increase of the barrier width. Nevertheless this method saturates at high barrier width due to the residual impurities in the barrier. Moreover, increasing barrier thickness is at the expense of an optimized electromagnetic field- quantum well overlap due to the coupling gratings. Nevertheless, in the following we have investigated the effect of the barrier width on the scattering reduction resulting from the doping shift, see FIG. 7. From this figure we can see that the larger the barrier, the larger the doping shift effect. This means that this method of doping shift will be particularly efficient in larger barrier QWIP.

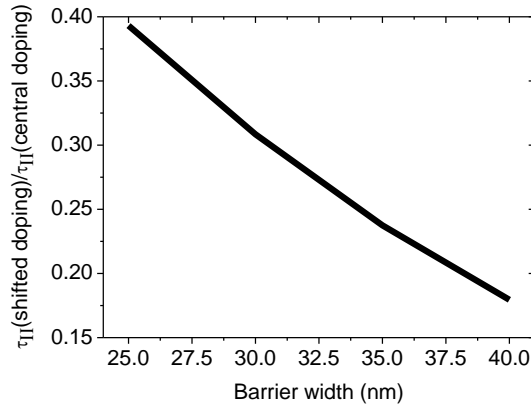


FIG. 7 Ratio of the scattering rate for a shifted doping and for a central doping as a function of the barrier width, for a null initial momentum.

Moreover, we have identified at least two other very common cases where our doping shift method may be applied (i) First in mid infrared quantum cascade detector^{24,25}, the R_0A (product of the resistance of the device under null bias by the area of the pixel) value is limited by the electron-impurities scattering²⁶, shifting the doping will allow an increase of the R_0A . (ii) In bicolor QWIP the operating temperature is generally determined by the longest wavelength device, making that the lowest wavelength device generally has this dark current operating in the tunnel regime. We underline that the range of application of the quantum scattering engineering is far larger than QWIP operating at low temperature.

VI. Conclusion

To conclude we have proposed and tested an alternative way to the barrier width increase for the reduction of the dark current in the tunnelling regime. This technique is based on the quantum scattering engineering of the interwell scattering rate. This results in the minimization of the scattering overlap integral between electron states in adjacent QWs by a shift of the doping position towards the border of the QWs. This method allows a reduction of 50 % of the tunnelling current while keeping the quantum efficiency almost unchanged. It is important to understand that our technique is beyond the simple use of QWIP at low temperature.

Reference

-
- ¹ A. Rogalski, J. Antoszewski and L. Faraone, *J. Appl. Phys.* **105**, 091101 (2009).
 - ² S. Bandara, S. Gunapala, S. Rafol, D. Ting, J. Liu, J. Mumolo, T. Trinh, A.W.K. Liu and J.M. Fastenau, *Infrared phys. Tech.* **42**, 237 (2001).
 - ³ H. Martijn, A. Gromov, S. Smuk, H. Malm, C. Asplund, J. Borglind, S. Becanovic, J. Alverbro, U. Halldin and B. Hirschauer *Inf. Phys. Tech.* **47**, 106 (2005).
 - ⁴ M. Z. Tidrow, *Mater. Sci. Eng. B* **74**, 45 (2000).
 - ⁵ A. Nedelcu, V. Guériaux, A. Bazin, L. Dua, A. Berurier, E. Costard, P. Bois and X. Marcadet, *Infrared phys. Tech.* **52**, 412 (2009).
 - ⁶ H. Schneider and H.C Liu, in *Quantum well infrared photodetectors*, Springer, Berlin, 2007.
 - ⁷ E. Lhuillier, I. Ribet-Mohamed, E. Rosencher, A. Nedelcu and V. Berger, *Phys. Rev. B* **81**, 155305 (2010).
 - ⁸ R.Rehm, H. Schneider, M. Walther and P. Koidl, *Appl. Phys. Lett.* **80**, 862 (2002).
 - ⁹ H. Schneider, C. Shonbein, R.Rehm, , M. Walther and P. Koidl, *Appl. Phys. Lett.* **88**, 051114 (2006).
 - ¹⁰ E. Luna, A. Guzman, J.L. Sanchez-Rojas, E. Calleja and E. Munoz, *Infrared phys. Tech.* **44**, 383 (2003).

-
- ¹¹ E. Luna, Á. Guzmán, J.L. Sánchez-Rojas, J. M. Sánchez and E. Muñoz, *IEEE J. Sel. Top. Quant. Electron.* **8**, 1077 (2002).
- ¹² E.B.Dupont, D. Delacourt, D. Papillon, J.P. Schnell and M. Papuchon, *Appl. Phys. Lett.* **60**, 2121 (1992).
- ¹³ J.L. Pan, L.C. West, S.J. Walker, R.J. Malik and J.F. Walker, *Appl. Phys. Lett.* **57**, 366 (1990).
- ¹⁴ T. Unuma, M. Yoshita, T. Noda, H. Sakaki and H. Akiyama, *J. Appl. Phys.* **93**, 1586 (2003).
- ¹⁵ P. Harrison, in *Quantum wells, wires and dots: Theoretical and Computational Physics of Semiconductor Nanostructures*, first edition (Wiley interscience, Chichester UK, 2000)
- ¹⁶ C. Sirtori, F. Capasso, J. Faist, and S. Sandro, *Phys. Rev.B* **50**, 8663 (1994)
- ¹⁷ R. Ferreira and G. Bastard, *Phys. Rev. B* **40**, 1074 (1989)
- ¹⁸ T. Unuma, M. Yoshita, T. Noda, H. Sakaki, and Akiyama, *J. Appl. Phys.* **93**, 1586 (2003).
- ¹⁹ K. Seeger, in *Semiconductor Physics* 8th edition, Springer, Berlin, 2002 K. Seeger, in *Semiconductor Physics* 8th edition, Springer, Berlin, 2002.
- ²⁰ G. Bastard, in *Wave mechanics applied to semiconductor heterostructures*, les editions de physique, les Ulis, 1992.
- ²¹ C. Weisbuch and B. Winter, in *Quantum semiconductor structures*. Academic press, Inc, London, 1991.
- ²² J. Faist, F. Capasso, C. Sirtori, D. L. Sivco, A. L. Hutchinson, S. Nee G. Chu, and A. Y. Cho *Appl. Phys. Lett.* **65**, 94 (1994);
- ²³ A. Gomez, V. Berger, N. Péré-Laperne and L.D. Vaulchier, *App. Phys. Lett.* **92** (2008), 202110.
- ²⁴ L. Gendron, M. Carras, A. Huynh, V. Ortiz, C. Koeniguer, V. Berger, Quantum cascade photodetector, *Appl. Phys. Lett.* **85**, 2824 (2004).
- ²⁵ D. Hofstetter, M. Beck, J. Faist, Quantum cascade-laser structures as photodetectors, *Appl. Phys. Lett.* **81**, 2683 (2002).
- ²⁶ F.R. Jasnot, N. Péré-Laperne, L.A. Devaulchier, M. Carras, A. Buffaz and V. Berger, to be published.